

Oxidation and reduction of carcinogenic organic pollutants using ethylene glycol intercalated Fe:Cu LDH and its magnetic property

Sonika Panghal

Sharda University School of Basic Sciences and Research

Pankaj Gupta (✉ pankaj.chemistry2019@gmail.com)

Sharda University School of Basic Sciences and Research <https://orcid.org/0000-0003-2795-7235>

Richa Tomar

Sharda University School of Basic Sciences and Research

Research Article

Keywords: Powder X-ray diffraction, Magnetism, Catalytic oxidation, Catalytic reduction, Layered double hydroxide, Intercalation

Posted Date: February 7th, 2022

DOI: <https://doi.org/10.21203/rs.3.rs-1323471/v1>

License:   This work is licensed under a Creative Commons Attribution 4.0 International License.

[Read Full License](#)

Abstract

The goal of this study is to use a solvothermal approach to make ethylene glycol intercalated Fe:Cu (2:1) LDH. In the presence of an ethylene glycol medium, a solvothermal reaction of FeCl₃ with urea produced a brown powder. LDH was studied using a variety of analytical techniques with the goal of obtaining a large surface area for catalytic oxidation and reduction of carcinogenic organic pollutants in water. The PXRD pattern shows the rhombohedral symmetry. Exothermic nature in the decomposition and combustion of intercalated ethylene glycol was observed in the thermogravimetric analysis and differential scanning calorimetric spectroscopy. Vibrational stretching and bending modes in the FTIR and the presence of an ethylene glycol molecule in the inter-layer gallery was confirmed by Raman spectra. Layered morphology of the LDH was observed in the FESEM. UV-visible spectra showed d-d transition corresponding to the iron and copper ion in the LDH. The BET surface area and pore size were 125 m²/g and 0.38 cc/g, respectively. High surface area and redox property of metal ions in the LDH made this material an excellent catalyst toward oxidation and reduction of organic pollutants. The bifunctional catalytic properties were shown toward methylene blue dye and *p*-nitroaniline. Excellent antiferromagnetic and ferromagnetic properties of the synthesized material were shown and discussed.

Introduction

Inorganic materials with organic groups have found tremendous application in the field of paints and pigment by modifying their surface properties via surface hydroxyl group substitution [1]. The exceptional physiochemical characteristics of two-dimensional layered materials are of great interest [2]. Layered materials anisotropic structural properties make them potentially advantageous in a variety of applications, including optoelectronics, photonic, catalysis, piezoelectric, pollutant control and biomaterials [2–4]. Layered double hydroxide materials, also known as anionic clay, are a type of 2D layered material that has drawn a lot of attention in recent years. LDHs are made up of layers of positively charged octahedral coordination metal hydroxide that are sandwiched between two layers of intercalated anionic or solvated water molecules to neutralize the overall charge. The general formula of LDH: $[M^{2+}_{1-x}M^{3+}_x(OH)_2]^{x+}(A^{n-})_{x/n} \cdot mH_2O$, comprises of divalent ion: M^{2+} , trivalent ion : M^{3+} and A^{n-} is the interlayer anion [5, 6].

Organic pollutant with toxicity has posed a number of environmental risks, particularly when released into the environment alongside industrial waste [7–9]. Photocatalytic, catalytic oxidation, catalytic reduction, adsorption, biological treatment and other approaches have all been used to remove contaminants [10]. These procedures, however, have significant drawbacks, such as sluggish process, secondary pollutant, high expense, and so on. Due to their great oxidation capacity, fast reaction rate, and wide application in the degradation of organic pollutants, advanced oxidation processes (AOPs) have gotten a lot of attention in the previous [11]. AOPs reduce organic pollutants by generating extremely reactive radicals; for example, the Fenton reaction generates hydroxyl radical (OH•) which is utilized to degrade organic pollutant into simple molecules and is one form of AOPs [12]. Similarly, reduction of organic nitroaromatics is chemically important in the industry as well as for environmental benefits [13–16]. The

reduction of nitroaromatics is the facile route to the synthesis of amino-aromatics, which is an intermediate several nitrogen containing compounds synthesis such as polymers cosmetics, agrochemicals, pesticides, pharmaceuticals, dyes, etc [17–19]. Several toxic, *p*-nitroanilines cause serious environmental pollutions. Nevertheless, can be converted into harmless *p*-aminoaniline which is a potential intermediate in pharmaceutical industry [20]. LDHs with hydrotalcite-like structure have been widely used in the field of adsorption, photocatalysis, organic conversion, etc [21–23]. LDHs as catalyst have gained sustainable interests in AOPs owing to its unique structure and its advantages [24]. High surface area of LDH provides massive active sites for organic pollutant which can speed up the oxidation reaction. The unique characteristic of LDHs is that, it often been used for the accelerating the degradation process of organic pollutants [25].

In the present report, ethylene glycol intercalated Fe:Cu (2:1) LDH is synthesized by solvothermal treatment of FeCl₃, CuCl₂.2H₂O and urea in ethylene glycol. Concurrently, consequences of this LDH in term of catalytic oxidation, catalytic reduction and magnetic properties have been studied in detail.

Materials And Characterization

2.1 Synthesis

FeCl₃ (99.9%, Thomas Baker), ethylene glycol (Merck, 99%), CuCl₂.2H₂O (99%, Merck) and urea (99%, Qualikem) were used, 3.24 g of FeCl₃ (2 mmol), 1.70 g of CuCl₂.2H₂O (1 mmol) were dissolved in 10 mL of ethylene glycol (EG) to which 1.80 g of urea (3 mmol) was added. The resulting solution was then agitated for 15 minutes using a magnetic stirrer before being transferred to 55 mL autoclave. The autoclave was filled with 18 mL of ethylene glycol before being sealed and heated at 160 °C for 24 hours. The product was rinsed many time with a mixture of double distilled water and alcohol (50:50) volume.

2.2 Characterization Techniques

Thermo gravimetric (TG) analysis of xerogels was performed on a NETZSCH STA-449 F3 instrument with a heating rate of 10°C/min in the temperature range of 30-1000 °C. A high-resolution Bruker D-8 Advance X-ray diffractometer was used to record the powder X-ray diffraction (PXRD) pattern. Raman spectra were collected using a Renishaw spectrometer and a microscopic setup with an Ar⁺ laser ($\lambda = 532$ nm) that was used for 20 MW-5000 hours. ZEISS Gemini SEM 500 was used to capture SEM images. Using BaSO₄ as a reference, diffuse reflectance spectra of the materials were acquired using a Perkin-Elmer Lambda-35 UV-visible spectrophotometer with an integrated sphere connected to it. Built software was used to convert the data to absorbance. At room temperature, a vibrating sample magnetometer (Microsense EV9, Lowell, MA) was used to assess magnetization. Low temperature magnetic measurement was taken using then MPMS (Magnetic Properties Measurement System) excel manufacturing quantum design USA in the temperature range of 1.8 to 320 K with a ± 1 Tesla applied field.

2.3 Catalytic experiment

For the catalytic oxidative studies methylene blue (MB) was used, with 30 mg of the ethylene glycol intercalated Fe:Cu (2:1) LDH was added to the three different solutions containing 50 mL of 50 μ M, 100 μ M and 200 μ M methylene blue, and 2 mL of 30% H₂O₂. To carry out the reduction reactions, 30 mg of the sample was added to the three different solutions containing 50 mL of 100 μ M, 200 μ M and 300 μ M *p*-nitroaniline with 50 mL of NaBH₄ (5.2×10^{-3}).

Results And Discussion

PXRD pattern of ethylene glycol intercalated Fe:Cu (2:1) layered double hydroxide has been presented in Fig. 1(a). The layered structure of the sample where ethylene glycol is being intercalated between in inter gallery was indicated in the PXRD pattern. The inter gallery expansion from 7.50 to 10.72 Å using ethylene glycol medium suggested monolayer of ethylene glycol molecule. The observed PXRD pattern of ethylene glycol intercalated Fe:Cu (2:1) layered double hydroxide was successfully indexed in the rhombohedral symmetry with $a = 3.175$ and $c = 31.9$ Å. The ethylene glycol intercalation was studied thoroughly in our previous publication [26]. The intercalated ethylene glycol moiety was further confirmed by thermogravimetric analysis (Fig. 1(b)). The initial weight loss at around 160 °C was attributed to the water molecules adsorbed on the surface, the weight loss observed between 180 °C to 250 °C was corresponding to the surface adsorbed and interlayered ethylene glycol molecules. Drastic weight loss from 250 °C to 330 °C was observed to the combustion of ethylene glycol as well as dihydroxylation of lattice [27, 28], the exothermic nature was shown in its DSC trace [29]. Intercalation of ethylene glycol moiety was further confirmed by FTIR and Raman spectra (Fig. 1(c) and (d)), respectively. The intense band at 3363 and 1612 cm⁻¹ could be attributed to the stretching and bending vibrations of hydroxide group, the band at lower wavenumber for hydroxide group usually reported for layered double hydroxide sample with any organic intercalant. The intercalated ethylene glycol molecule could shift the band in FTIR due to the decreasing bond order of O and H. The band at 2858, 1451, 1110, 1038, 897, 1288 cm⁻¹ were corresponding to the C-H asymmetrical stretching, C-H, symmetrical stretching, C-O-H bending CH₂ rocking and C-O stretching vibration of the intercalated ethylene glycol, respectively [27, 29, 30, 31]. The band at lower wavenumber 2905 and 2858 cm⁻¹ for C-H stretching vibration modes strongly supports the intercalation in the interlayer. The vibration modes at 626 and 446 cm⁻¹ could be attributed to the M-O units [32]. In Raman spectra, bands at 340, 410, 450, 640, 900, 1222 and 1315 cm⁻¹ were corresponding to the C-C-O (bending), CH₂ (rocking), C-C (stretching), C-O (stretching), bending, wagging and vibration mode of CH₂ belonging to ethylene glycol units. Extra bands at 190 and 236 cm⁻¹ were corresponding to the M-O lattice vibrations [33, 34]. A sheet like morphology was observed in the FESEM image (Fig. 1(e)) which confirmed the layered structure of the ethylene glycol sample. The absorbance spectra of the ethylene glycol intercalated Fe:Cu (2:1) LDH was shown in Fig. 1(f). On deconvolution, the bands at 217, 255, 337, 406, 472, 620 and 836 nm were corresponding to the *d-d* transition of Fe and Cu. Low band at 217, 255 and 337 nm were corresponding to the LMCT and ²B_{1g} → ²E_g transition of Cu. The bands at 406, 472 and 836 nm were corresponded to the ⁶A₁ + ⁶A₁ → ⁴T₁ (⁴G) + ⁴T₁ (⁴G), ⁶A₁ → ⁴E and ⁶A₁ → ⁴T₁ (⁴G) transition. Band at 620 nm was attributed to the CT band of Fe (II) to Fe (III) [35]. The broad band between 700 to 850 nm also corresponded to the ²B_{1g} → ²B_{2g} in octahedral coordination of Cu. Layered

double hydroxide materials are extensively used as a catalyst for oxidation of various carcinogenic dyes and organic transformations. The mechanism of these transformation involve adsorption of organic compound on the surface of catalyst, so before examine the sample as a catalyst, the surface area and pore volume of ethylene glycol Fe:Cu (2:1) LDH was analyzed by the BET method.

The BET plot was shown in Fig. 2. The surface area and pore volume for the ethylene glycol intercalated Fe:Cu (2:1) layered double hydroxide was found to be 125 m²/g and 0.38 cc/g, respectively. The high surface area could be obtained by the evolution of gases during synthesis [26, 27]. The catalytic oxidation of methylene blue dye under hydrogen peroxide in presence of ethylene glycol intercalated Fe:Cu (2:1) LDH sample has been presented in Fig. 3.

Different concentrations of MB dye were taken along with 2 mL of hydrogen peroxide. Drastic reduction in the intensity of the absorbance peak was observed after addition of catalyst. In the absorbance plot, clearly indicate the decrease in absorbance efficiency with increasing concentration of dye. At low concentration of 50 μM, 85% of the dye got degraded in 10 minutes and it increased to 97% in 60 min. While at 100 μM and 200 μM, 92% and 87% of MB dye was degraded in 60 minutes. The expression used to analyze the degradation kinetics was

$$C_t = C_o \exp(-kt)$$

Where C_o and C_t represent the initial and final concentration of dye at time t, respectively, t denotes the time of reaction, k is the pseudo first order rate constant. The comparison of rate constant of MB dye was shown in Table 1

Table 1
The comparison of 'k' values obtained for the catalytic oxidation of MB dye.

Dye concentration	Rate constant 'k' (min ⁻¹)
50 μM	6.1 × 10 ⁻²
100 μM	5.4 × 10 ⁻²
200 μM	3.4 × 10 ⁻²

The observed rate constant for oxidation of 100 μM MB dye was lower than our previous literature report, low surface area of present catalyst as compare to ethylene glycol intercalated Fe(II)-Fe(III) LDH might decreased the catalytic efficiency toward oxidation. To check out the regeneration of catalyst, cyclic experiments were carried out, this regeneration of catalyst is extensively used in the industries. The recyclability experiment of 50 μM MB dye in presence of ethylene glycol intercalated Fe:Cu (2:1) LDH was shown in Fig. 3(e). The present sample showed its capability to catalyzed nearly 87% up to three cycles, after which it catalyzed only 73% of the dye molecule in the fourth time usage. The catalytic performance of the present sample was compared with the other literature reports have been compiled in Table 2.

Table 2

A comparison of values of rate constant obtained from catalytic oxidation of MB dye using various types of catalyst.

Catalyst	Concentration of methylene blue (M)	Rate constant (min ⁻¹)	Ref.
Fe ₃ O ₄	1.0 × 10 ⁻⁴	5.6 × 10 ⁻²	[36]
MgFe ₂ O ₄	1.0 × 10 ⁻⁴	4.2 × 10 ⁻²	[37]
MgCr ₂ O ₄	1.0 × 10 ⁻⁴	3.3 × 10 ⁻¹	[38]
EG Intercalated Fe ²⁺ /Fe ³⁺ LDH	1.0 × 10 ⁻⁴	2.8 × 10 ⁻¹	[26]
EG Intercalated Fe:Cu (2:1) LDH	5.0 × 10 ⁻⁵	6.1 × 10 ⁻²	Our work
EG Intercalated Fe:Cu (2:1) LDH	1.0 × 10 ⁻⁴	5.4 × 10 ⁻²	Our work
EG Intercalated Fe:Cu (2:1) LDH	2.0 × 10 ⁻⁴	3.4 × 10 ⁻²	Our work

The ethylene glycol intercalated Fe:Cu (2:1) LDH in our system examined its utility towards the catalytic reduction of carcinogenic nitro organic substrates. Nitro compounds are usually obtained as a byproduct in the pharmaceutical, agrochemicals, urethane polymer and dye industries. As a result, researcher are working hard to convert nitro aromatics into more usable amino compounds utilizing a variety of catalytic system [17–20]. The reaction was monitored using UV-visible spectrum followed by typical transition associated with this molecule. The results for the reduction reaction of *p*-nitroaniline was shown in Fig. 4. The typical absorbance band for *p*-nitroaniline was observed at 381 nm in UV-visible spectrum. A decreasing absorption band at 381 nm along with the simultaneous appearance of new band at around 300 nm was observed within 5 minute in the presence of ethylene glycol intercalated Fe:Cu (2:1) LDH which was suggested for the appearance of *p*-aminophenol [39].

Catalytic rate was decreased with increasing the concentration of *p*-nitroaniline (Fig. 4(d)), the rate constant in presence of our catalyst was compiled in Table 3.

Table 3

The comparison of 'K' for the reduction *p*-nitroaniline at different concentration

<i>p</i> -nitroaniline concentration (μM)	Rate constant 'K' (min ⁻¹)
100	2.77 × 10 ⁻¹
200	2.19 × 10 ⁻¹
300	1.64 × 10 ⁻¹

Catalytic activity of present catalyst with other literature reports have been compiled in Table 4.

Table 4
The comparison of 'K' for the reduction of *p*-nitroaniline with various other catalyst

Catalyst	Concentration of <i>p</i> -nitroaniline (M)	Rate constant 'K' (min ⁻¹)	Ref.
CuO	1.0×10^{-3}	7.50×10^{-3}	[40]
Ag porous glass hybrid composite	1.0×10^{-3}	1.23×10^{-1}	[41]
Au Nanoparticles	3.0×10^{-4}	0.87×10^1	[42]
Gold Nanoparticles	1.0×10^{-3}	4.50×10^{-2}	[43]
EG-Intercalated Fe ²⁺ /Fe ³⁺ LDH	1.0×10^{-4}	1.57×10^{-1}	[26]
EG-Intercalated Fe:Cu (2:1) LDH	1.0×10^{-4}	2.77×10^{-1}	Our work
EG-Intercalated Fe:Cu (2:1) LDH	2.0×10^{-4}	2.19×10^{-1}	Our work
EG-Intercalated Fe:Cu (2:1) LDH	3.0×10^{-4}	1.64×10^{-1}	Our work

Up to three cycles of reuse, the catalyst maintained its efficiency and further use could reduce the catalytic rate of conversion. The rate constant for the conversion of nitro compound to amino compound in cyclic experiment in the presence of our catalyst is compiled in Table 5.

Table 5
Comparative rate constant for cyclic experiment of *p*-nitroaniline

Cycle	Rate constant (min ⁻¹)
1st cycle	2.77×10^{-1}
2nd cycle	2.47×10^{-1}
3rd cycle	1.65×10^{-1}
4th cycle	1.30×10^{-1}

The results concluded that the, catalytic conversion efficiency was faster for the 1st cycle and it was decreased as the number of cyclic increased. The PXRD pattern results confirmed the stability and refuse the major structure change after reuse.

In Fig. 5(a), magnetization as a function of magnetic field at 300 K for ethylene glycol intercalated Fe:Cu (2:1) LDH has been plotted. The S shape curve of magnetization with narrow hysteresis loop suggested the antiferromagnetic ordering in the sample at room temperature [43]. This could be due to the overlapping of one unpaired spin in the copper. For further magnetic study in the layered double hydroxide sample, low temperature magnetism has been carried out. Magnetic susceptibility of ethylene glycol intercalated Fe:Cu (2:1) LDH in zero field cooled (ZFC) and field cooled (FC) at 1000 Oe have been plotted in Fig. 5(b). Antiferromagnetic ordering was observed in ZFC with Neel temperature of $T_N = 41.95$ K. Typical antiferromagnetic behavior of our sample was shown below Neel temperature and above T_N , it showed paramagnetic ordering. In case of field cooled (FC), typical ferromagnetic behavior was observed below curie temperature ($T_c = 91.58$ K), which suggested the existence of large domain in the same direction, afterward paramagnetic ordering was seen [44, 45]. An inhomogeneous mixture of ferromagnetic and antiferromagnetic ordering in ZFC and FC curve suggested the frustration in the ethylene glycol intercalated Fe:Cu (2:1) LDH.

Conclusions

An ethylene glycol intercalated Fe:Cu (2:1) layered double hydroxide was synthesized by the reaction between FeCl_3 , $\text{CuCl}_2 \cdot 2\text{H}_2\text{O}$ and urea using solvothermal method. The observed reflection peaks in powder X-ray diffraction pattern indicated the layered structure of sample where ethylene glycol is intercalated in the inter-layer gallery. Three step weight loss in the thermogravimetric analysis spectrum suggested the decomposition and combustion of surface adsorbed and intercalated ethylene glycol molecule. The observed bands in FTIR and Raman spectra suggested the vibrational stretching and bending modes of ethylene glycol molecule. Layered type morphology was clearly observed in the FESEM. High surface area (125 g/m^2) and pore volume (0.38 cc/g) was observed in the BET measurement. This layered sample was found to be an efficient catalyst for the oxidation of methylene blue dye as well as for the reduction of carcinogenic nitroaromatic compounds to biologically active amino compounds. The layered material showed antiferromagnetic property below T_N and ferromagnetic property below T_c . Inhomogeneous behaviour was also observed in the ZFC and FC plots.

Declarations

Acknowledgments

The authors thanks Sharda University for their support.

References

1. River V (2001) Layered double hydroxides: Present and future. Nova Science Publication Inc., New York
2. Wan J, Lacey SD, Dai J, Bao W, Fuhrer MS, Hu L (2016) Chem Soc Rev 45:6742–6765

3. Ma L, Wang Q, Islam SM, Liu Y, Ma S, Kanatzidis MG (2016) *J Am Chem Soc* 138:2858–2866
4. Ma S, Huang L, Ma L, Shim Y, Islam SM, Wang P, Zhao LD, Wang S, Sun G, Wang X (2015) *J Am Chem Soc* 137:3670–3677
5. Tao Q, Reddy BJ, He H, Frost RL, Yuan P, Zhu J (2008) *Mater Chem Phys* 112:869–875
6. Yu J, Wang Q, O'Hare D, Sun L (2017) *Chem Soc Rev* 46:5950–5974
7. de Souza SM, Bonilla KA, de Souza AA (2010) *J Haz Mater* 179:35–42
8. Drumond Chequer FM, de Oliveira GAR, Anastacio ER, Ferraz J, Carvalho MV (2013) *Boldrin Zanoni, Textile dyes: Dyeing process and environmental impact. Eco-friendly textile dyeing and finishing. InTech. Chapter 6,*
9. Du YB, Niu CG, Zhang L, Ruan M, Wen XJ, Zhang XG, Zeng GM (2017) *Mol Catal* 436:100–110
10. Qi C, Liu X, Liu C, Zhang H, Li X, Ma J (2017) *Chem Eng J* 315:201–209
11. Cheng M, Zeng G, Huang D, Lai C, Xu P, Zhang C, Liu Y (2016) *Chem Eng J* 1284:582–598
12. Yao Y, Mao Y, Huang Q, Wang L, Huang Z, Lu W, Chen W (2014) *J Har Mater* 264:323–331
13. Varma RS (2014) *Green Chem* 16:2027–2041
14. Goswami A, Rathi AK, Aparicio C, Tomanec O, Petr M, Pocklanova R, Gawande MB, Varma RS, Zboril R (2017) *Appl Mater Interfaces* 9:2815–2824
15. Dutta KJ, Rathi AK, Gawande MB, Ranc V, Zoppellaro G, Varma RS, Zboril R (2016) *Chem Cat Chem* 8:2351–2355
16. Kabalka GW, Laila GMH, Varma RS (1990) *Tetrahedron* 46:7443–7457
17. Blaser HU, Malan C, Pugin B, Spindler F, Steiner H, Studer M (2003) *Adv Synth Catal* 345:103–151
18. Ayad MM, Amer WA, Kopt MG (2017) *Mol Catal* 439:72–80
19. Datta KJ, Rathi AK, Kumar P, Kaslik J, Medrik I, Ranc V, Varma RS, Zboril R, Gawande MB (2017) *Sci Rep* 7:1–12
20. He S, Niu H, Zeng T, Wang S, Cai Y (2016) *Chem Select* 1:2821–2825
21. Shan R, Yan LG, Yang YM, Yang K, Yu SJ, Yu HQ, Zhu BC, Du B (2015) *J Ind Eng Chem* 21:561–568
22. Tokudome Y, Morimoto T, Tarutani N, Vaz PD, Nunes CD, Prevot V, Stenning GB, Takahashi M (2016) *ACS Nano* 10:5550–5559
23. Ganiyu SO, Huong Le TX, Bechelany M, Esposito G, Van Hullenusch ED, Oturan MA, Cretin M (2017) *J Mater Chem A* 5:3655–3666
24. Huang X, Su M, Zhou J, Shu W, Huang Z, Guo N, Qian G (2017) *Chem Eng J* 328:66–73
25. Zhang M, Yao Q, Lu C, Li Z, Wang W (2014) *Appl Mater Interfaces* 6:20225–20233
26. Nagarajan R, Gupta P, Singh P, Chakraborty P (2016) *Dalton Trans* 45:17508–17520
27. Wang C, Zhang X, Xu Z, Sun X, Ma Y (2015) *Appl Mater Interfaces* 7:19601–19610
28. Wang C, Zhang X, Sun X, Ma Y (2016) *Electrochim Acta* 191:329–336
29. Guimaraes JL, Marangoni R, Ramons LP, Wypych F (2000) *J Colloid Interface Sci* 227:445–451

30. Stanimirova T, Hibino T (2006) *Appl Clay Sci* 31:65–75
31. Kasai A, Fujihara S (2016) *Inorg Chem* 45:415–418
32. Xiao T, Tang Y, Jia Z, Li D, Hu X, Li B, Luo L (2009) *Nanotechnol* 20:475603–475610
33. Williams RM, Atalla RH (1975) *J Chem Soc Perkin Trans 2*:1155–1161
34. Luo RS, Jonas J (2001) *J Raman Spectrosc* 32:975–978
35. Hansen HCB (1989) *Clay Min* 24:663–669
36. Zhu M, Diao G (2011) *J Phys Chem C* 115:18923–18934
37. Tripathi VK, Nagarajan R (2016) *Adv Powder Technol* 27:1251–1256
38. Tripathi VK, Nagarajan R (2016) *J Am Ceram Soc* 99:814–818
39. Chiu CY, Chung PJ, Lao KU, Liao CW, Huang MH (2012) *J Phys Chem C* 116:23757–23763
40. Revathi K, Palantavinda S, Vijayan BK (2019) *Mater Today: Proceed* 9:633–638
41. Huang GG, Sou NL, Hung MJ (2016) *Spectrochim Acta A* 166:8–14
42. Gupta SSR, Kantam ML, Bhanage BM (2018) *Nanostruct Nanoobject* 14:125–130
43. Reddy V, Torati RS, Oh S, Kim C (2013) *Ind Eng Chem Res* 52:556–564
44. Carrasco JA, Silva AS-D, Oestreicher V, Romero J, Markus BG, Simon F, Vieira BJC, Waerenborgh JC, Abellan G, Coronado E (2020) *Chem Eur J* 26:6504–6517
45. Carrasco JA, Abellan G, Coronado E (2018) *J Mater Chem C* 6:1187–1198

Figures

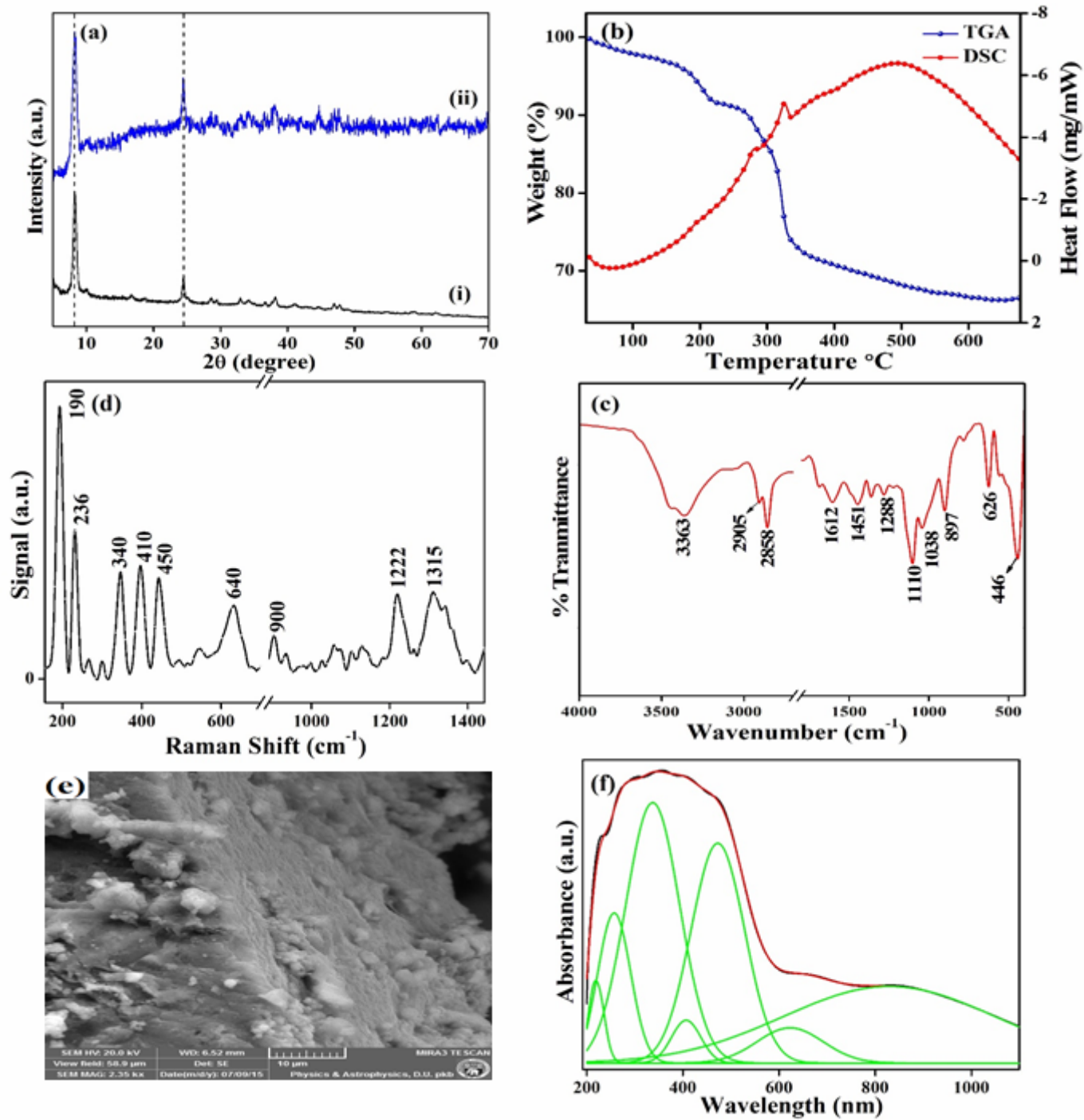


Figure 1

(a) PXRD pattern, (b) thermogravimetric and differential scanning calorimetric traces, (c) FTIR spectra, (d) Raman spectra, (e) FESEM image and (f) UV-visible spectra of ethylene glycol intercalated Fe:Cu (2:1) LDH.

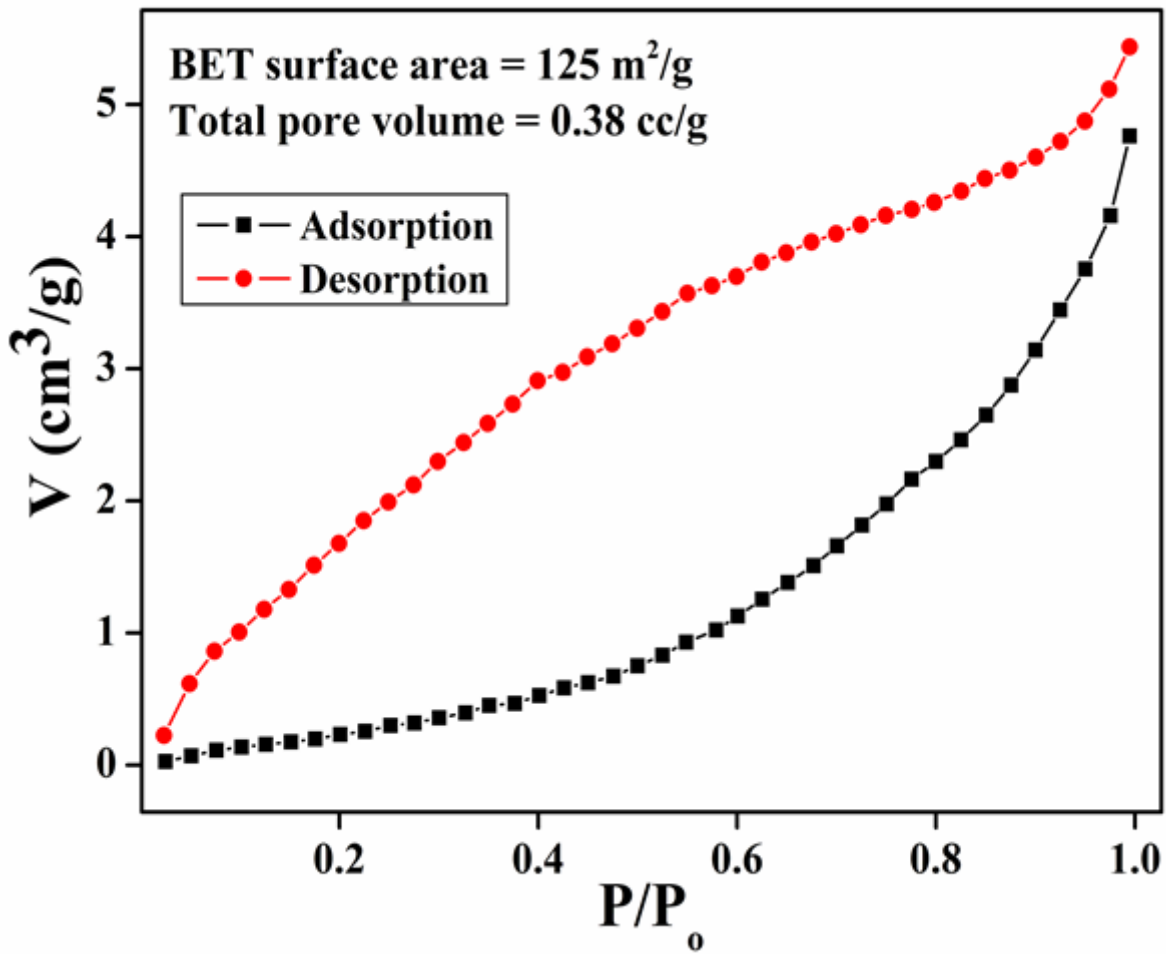


Figure 2

BET adsorption-desorption isotherm of ethylene glycol intercalated Fe:Cu (2:1) LDH.

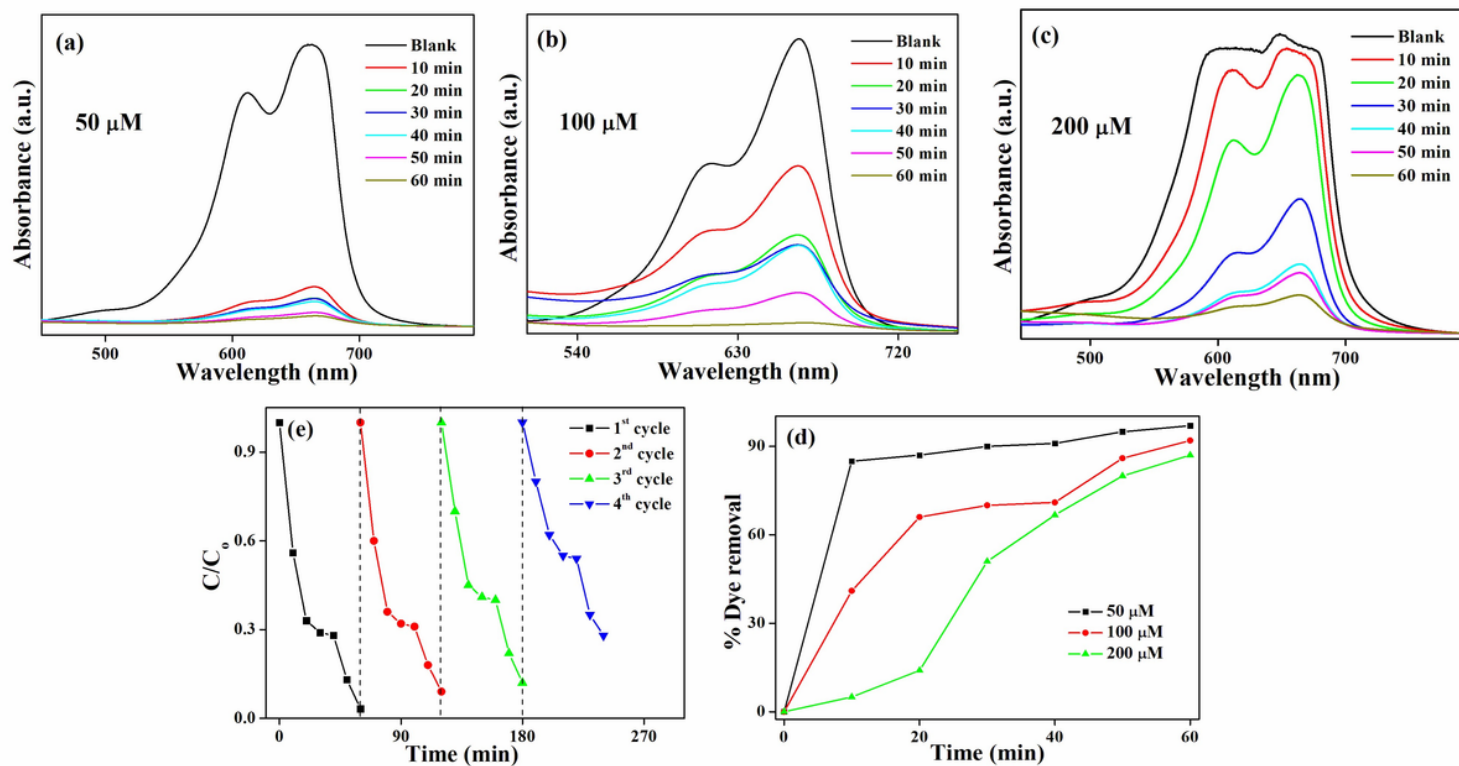


Figure 3

(a)-(c) Absorbance plot of MB dye in presence of H₂O₂ and 30 mg ethylene glycol intercalated Fe:Cu (2:1) LDH, (d) % dye removal versus time plot and (e) cyclic experiment of MB dye (50 μM).

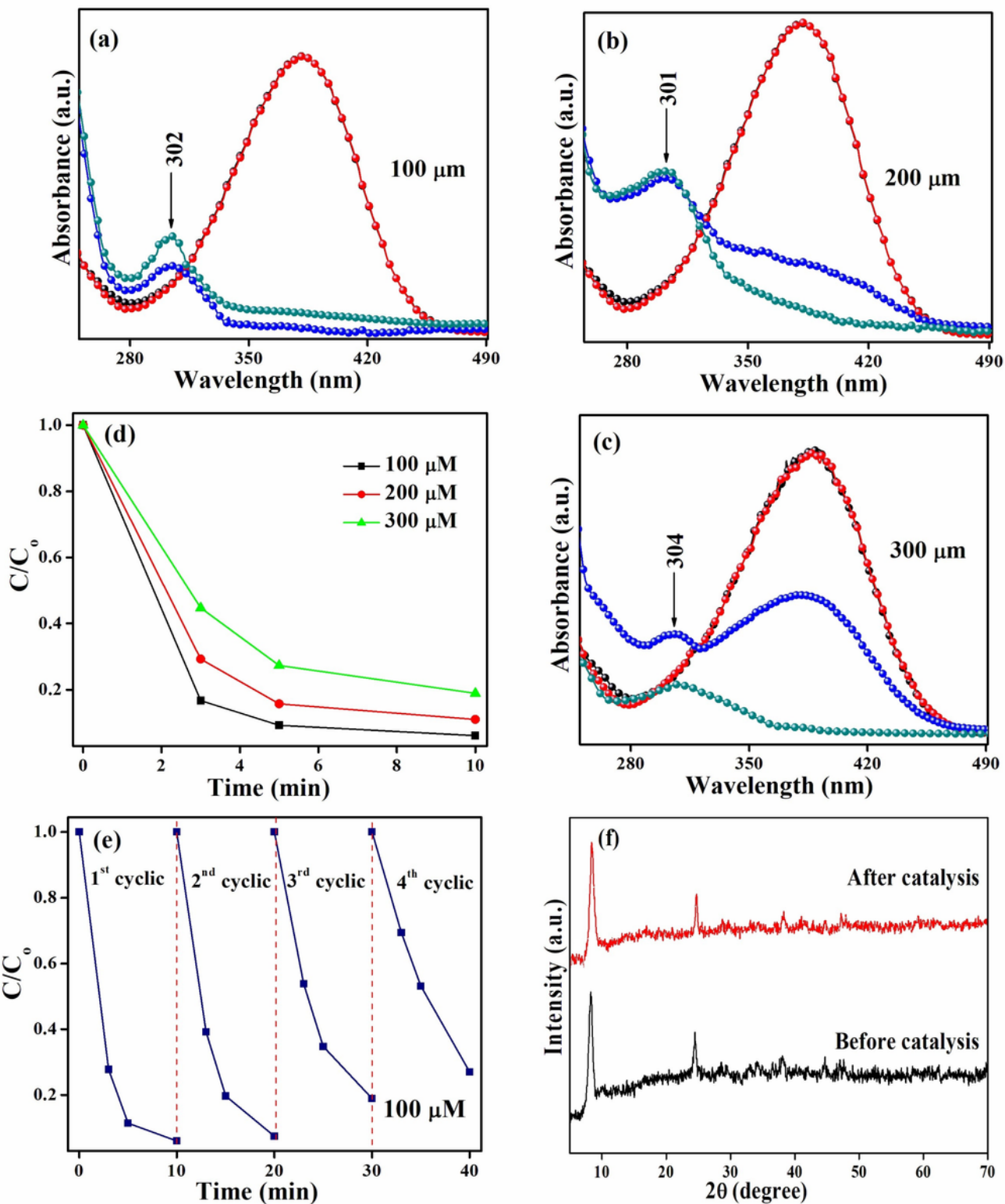


Figure 4

(a)-(c) UV-visible spectra of *p*-nitroaniline in presence of NaBH₄ and ethylene glycol intercalated Fe:Cu (2:1) LDH, (b) C/C_0 versus time plot, (d) recyclability plot and (f) powder x-ray diffraction pattern after its catalytic usage.

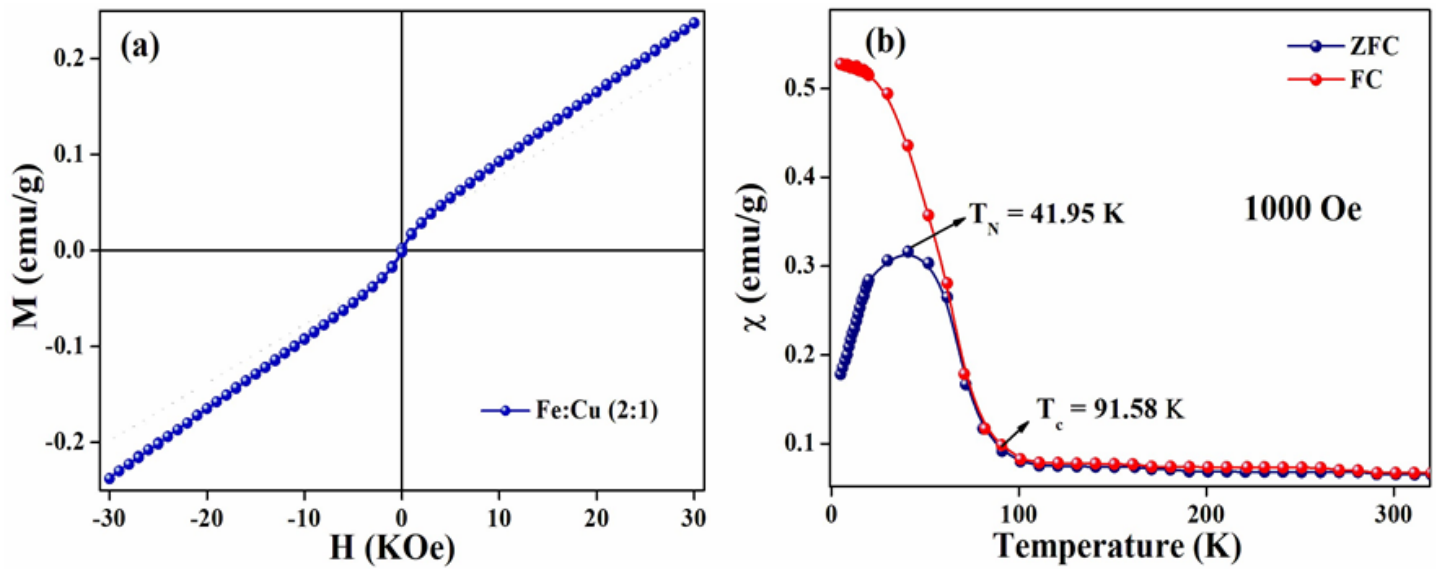


Figure 5

(a) M-H plot at 300 K and (b) variation of magnetic susceptibility with temperature under zero magnetic field and at an applied magnetic field at 1000 Oe for ethylene glycol intercalated Fe:Cu (2:1) LDH.